ELSEVIER

Applied Catalysis A: General 164 (1997) 21–33

APPLIED CATALYSIS A: GENERAL

Methane conversion to higher hydrocarbons in a corona discharge over metal oxide catalysts with OH groups

Changjun Liu, Abdulathim Marafee, Richard Mallinson, Lance Lobban*

Institute for Gas Utilization Technologies and School of Chemical Engineering and Materials Science, University of Oklahoma, 73019 Norman OK, USA

Received 16 September 1996; received in revised form 9 April 1997; accepted 11 April 1997

Abstract

The gas discharge promoted oxidative conversion of methane to higher hydrocarbons over various metal oxide and zeolite catalysts was investigated over a wide range of temperatures (373–973 K). The most significant gas discharge effects were observed over catalysts containing polar OH groups. Significant methane conversions and C_2 yields were achieved at temperatures sufficiently low that no intrinsic catalytic activity for C_2 production was found in the absence of gas discharge, and the lower the gas temperature, the greater was the observed gas discharge effect on methane conversion. It is believed that the gas discharge effects depend on the gas temperature, the concentration of the OH groups and the acidity and basicity of the OH groups on the catalysts. A possible reaction mechanism for gas discharge promoted catalysis is presented. © 1997 Elsevier Science B.V.

Keywords: Methane; Hydrocarbon; Catalysis; Gas discharge; Plasma; Metal oxide; Zeolite

1. Introduction

The oxidative coupling of methane (OCM) to higher hydrocarbons has become a subject of extensive research worldwide since the early 1980s. Due to the relatively stable nature of methane, however, catalytic conversion of methane typically requires high reaction temperatures (in excess of 973 K) to activate the catalyst. Such high temperatures increase the capital and energy costs of processes, and the high temperature decreases the C_2 selectivity via unselective gas phase combustion reactions. Much research has subsequently focused on lower temperature activation of methane, e.g., by low-temperature catalysts, by addition of steam into reactants, and by photochemical and microwave techniques. Since Lunsford and co-workers [1,2] reported lithium-doped magnesium oxide as an effective catalyst for OCM, alkali and alkaline earth metal compounds have been extensively investigated. Some of these catalysts, e.g., 5.3 wt% Li/MgO [3] and 50 wt% LiCl–50wt% Na_2MoO_4 [4] have been found to be active and selective for OCM at somewhat lower temperatures. Li et al. [5] reported their results of low temperature oxidative coupling of methane over a perovskite catalyst, $SiTiO_3$ doped with MgO. A high selectivity (over 90%) was achieved at 698 K. The catalyst activity was attributed to adsorbed

*Corresponding author. e-mail: llobban@ou.edu

PII S0926-860X(97)00154-3

oxygen ions at an oxide defect, which react directly with CH_4. For these catalysts, however, the yield of C_2 hydrocarbons was not sufficiently high. Addition of steam to the feed was found to increase methane conversion at temperatures less than 600°C over calcium–nickel–potassium oxide [6–8]. The presence of added steam was found to lower the temperature (<873 K) for oxidative coupling of methane (OCM) over Li/MgO. Methane steam reforming sometimes became dominant, however, and catalyst stability was a problem. A potentially significant improvement in OCM is the application of photochemical and electric field techniques. Zhong and Ma [9] used a CO_2-pulsed laser to irradiate methane and air on a $LiClO_4$/$Pb_3(PO_4)_2$ composite solid surface. They achieved 35% methane conversion with 93% ethylene selectivity at 473 K. Other products are ethane and propane. For the photochemical conversion, the photon is an energy carrier. Photochemical conversion can be highly selective because the photon energy can be more sharply defined and the photonic cross-section is significantly smaller than the electronic. However, one can generate electrons much more efficiently than photons. Therefore, an electrochemical or plasma chemical method may be more efficient and effective than a photochemical technique. Chen et al. [10] presented their results of methane conversion using microwave heating in place of a furnace over proton conductive catalysts. When the catalyst is a good dielectric material, it is easy to convert electromagnetic energy into heat. The reaction temperature for methane conversion with microwave heating was 200 K less than required with the regular furnace heating when the selectivity and yield of C_2 were almost the same [10]. Apart from simple microwave heating of the catalyst, when the voltage of the electric field is sufficiently high, a microwave plasma can be initiated in the gas phase. Suib et al. [11] achieved a lower reaction temperature for methane conversion using microwave plasma-promoted catalysis. They placed catalysts in the post-plasma zone so that the active species formed during plasma reactions came into direct contact with the catalysts. Good results were achieved using a Ni powder catalyst at temperatures below 698 K. Non-oxidative methane conversion was as high as 52% with selectivities to ethane 50%, ethylene 25% and acetylene 25%. There was no positive plasma effect found with typical catalysts, such as Sm_2O_3 and Li/MgO.

It is well known that the electronic properties of catalysts have an important role in OCM [12]. The electronic properties, and therefore catalytic properties, can be expected to change if the catalyst is electrically charged. Here, we report our recent results in oxidative methane conversion over charged catalysts within DC streamer corona discharges.

2. Experimental

2.1. DC streamer corona discharge

DC streamer corona discharge is a cold (non-equilibrium) plasma phenomenon. It can be initiated at atmospheric pressure using inhomogeneous electrode geometries, such as the wire-and-plate electrode configuration shown in Fig. 1. During the DC streamer discharge reactions, the gas discharges were formed in a gap between two stainless steel electrodes. The top wire electrode was a 1/16 in. stainless steel rod concentric with the center of the reactor tube, while the lower grounded electrode was a circular disk positioned perpendicular to the reactor axis and 10 mm below the tip of the top wire electrode when the remote discharge was employed (Fig. 1a) or 6 mm below when the direct discharge was employed (Fig. 1b). The catalyst bed was about 8 mm deep, thus the tip of the wire electrode was about 2 mm above the top of catalyst bed for the remote discharge and about 2 mm within the bed for the direct discharge. The catalyst powder (40–60 mesh) is electrically charged by the streamer corona discharge.

2.2. Catalyst preparation and characterization

Catalysts included La_2O_3, CeO_2, Li/MgO, Sm_2O_3, Sr–La_2O_3/$La(OH)_3$ and CaO/NaOH, as well as zeolite catalysts NH_4Y, Na–ZSM-5, NaOH-treated Y. All these catalysts except zeolites have shown some activity for OCM in the absence of gas discharge [12]. All catalysts used were in powder form. For catalyst characterization, the powder diffraction analysis (XRD) of the solid sample was performed with a Rigaku Geigerflex Diffractometer using filtered CuKα

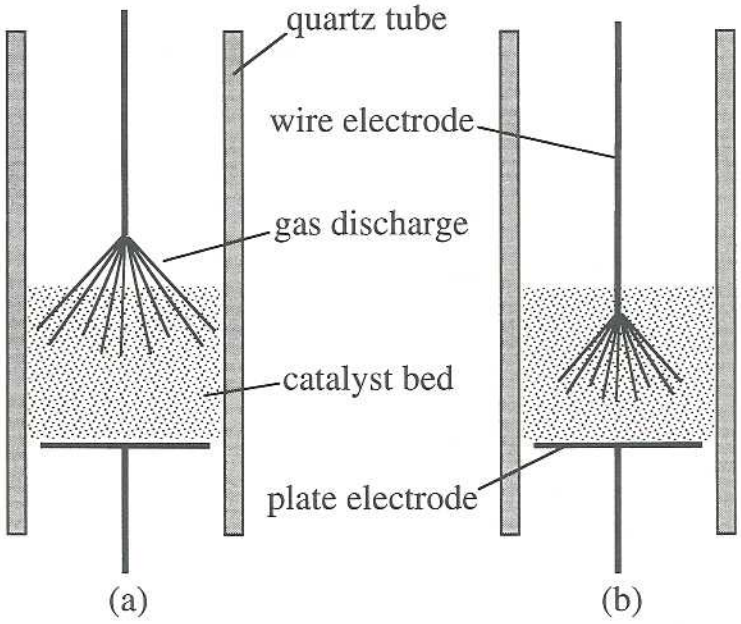

Fig. 1. Schematics of corona discharge reactor system: (a) Remote discharge, (b) direct discharge.

radiation. Surface analysis was carried out using a Perkin-Elmer PHI 1600 X-ray photoelectron spectrometer (XPS). Surface area analyses were carried out on a Micromeritics, ASAP 2100 Surface Area Analyzer.

For the preparation of catalysts, high-purity grade reagents were used as starting compounds. The powders of La_2O_3, CeO_2 and Sm_2O_3 purchased from Aldrich were used as received for the experimental studies. The preparation of Li/MgO has been described by Lobban et al. [13,14]. The CaO/NaOH catalyst was prepared by using calcium oxide impregnated with a solution of 10 wt% sodium hydroxide and dried at 373 K and then calcined in air at 573 K for 3 h. The $Sr–La_2O_3/La(OH)_3$ catalyst was prepared using the Pechini method as described in detail by Ajmera [15]. XRD characterization of this fresh catalyst indicated the catalyst to be approximately 30% $La(OH)_3$ and 68% La_2O_3. The BET surface area of this catalyst was found to be ca. 10 m^2/g. The Na–ZSM-5 zeolite was obtained from Chemie Uetikon and was used as received. NaOH treated Y zeolite was prepared using a commercial NH_4Y zeolite (Aldrich Chemical Company). The parent NH_4Y zeolite was immersed in a 1 M NaOH solution at room temperature for 8 h, during which the mixture was stirred frequently. The sample was then washed with deionized water and dried for 3 h at 423 K. The dried zeolite was calcined in air for 2 h at 773 K. XPS analyses of the prepared catalyst and the parent zeolite are reported in Table 1. The analyses indicate a large decrease in surface Si/Al caused by the NaOH treatment. However, the XRD analysis shows no change in the principal zeolite phase.

Table 1
XPS analysis of surface compositions of Y zeolites (atom%)

Sample	Al	Si	C	Na	O	N	Si/Al
NH4Y	8.98	16.42	31.90	0.31	41.36	1.03	1.83
Fresh Y (1 M NaOH treated)	26.16	3.46	17.94	0.23	52.21	0.00	0.13
Used Y (1 M NaOH treated)	25.96	4.13	16.73	0.37	52.81	0.00	0.16

2.3. Flow-system for experimental studies

The experimental apparatus flow diagram has been described in previous papers [16,17]. The quartz tube reactor with an i.d. of 7 mm was heated by a cylindrical furnace placed around the reactor. Methane and oxygen were mixed with the dilution gas, helium, to maintain a constant total flow rate and then introduced downward through the reactor for all experiments. The flow rates of the feed gases methane, oxygen and helium were regulated by three Porter Instrument model 201 mass flow controllers. The feed was analyzed by on-line gas chromatography (HP 5890 equipped with a molecular sieve packed column and a thermal conductivity detector). The exhaust gas from the reactor was introduced into a condenser cooled by a mixture of dry ice and acetone which was used to remove the produced water. The effluent gas from the condenser was also analyzed by gas chromatography. The condensate was analyzed using a GCD system (HP GCD G1800A) using an electron ionization detector.

2.4. Temperature measurements

The streamer corona discharge is characterized by low bulk gas temperature and high electronic temperature or energy. The average electron energy is less than 6 eV [18] in the corona discharge. The gas temperature is important in determining the selectivity of products formed both homogeneously and heterogeneously in the corona discharge reactor. Gas phase temperature measurement, however, is complicated by the silent discharge which can occur between the wire electrode and a thermocouple if the thermocouple is too close to the electrode tip. Such a silent discharge would restrict the plasma to a small volume around the thermocouple tip, which would decrease the active volume for the discharge reactions. Therefore, the inner thermocouple was removed during our experiments. A thermocouple attached to the reactor outside wall was used to monitor gas temperature. A temperature calibration was performed first to ensure the accuracy of temperature measurements, and has been described elsewhere [16,17].

3. Results

3.1. $Sr–La_2O_3/La(OH)_3$

In our previous paper [17] we reported that the corona discharge enhances the oxidative conversion of methane to higher hydrocarbons over $Sr–La_2O_3/La(OH)_3$ catalyst. Compared to the catalytic process in the absence of corona discharge, a higher methane conversion and a higher C_2 product yield were achieved even at temperatures at which there is no C_2 activity for the catalyst alone. We believe that OH groups in the metal oxide catalyst are important for the enhancement. The typical OCM catalysts La_2O_3, CeO_2 and Sm_2O_3 showed no enhancement in the

Table 2
Gas discharge promoted catalytic conversion of methane over $Sr–La_2O_3/La(OH)_3$

Catalyst present	Gas discharge present	Gas temperature (K)	CH_4/O_2	CH_4 conversion (%)	O_2 conversion (%)	C_2 selectivity (%)	C_2 yield (%)
Yes	No	873	20/5	8.77	66.3	26.8	2.4
Yes	Yes	873	20/5	17.2	91.8	37.5	6.5
No	Yes	873	20/5	4.7	21.4	46.3	2.2
Yes	No	823	20/5	1.9	35.8	10.1	0.6
Yes	Yes	823	20/5	18.0	93.5	44.5	8.0
No	Yes	823	20/5	4.1	16.0	58.1	2.4
Yes	No	873	20/10	18.6	53.1	9.6	1.8
Yes	Yes	873	20/10	33.0	96.8	24.0	7.9
No	Yes	873	20/10	5.1	15.6	45.7	2.3
Yes	No	823	20/10	8.8	12.3	0.0	0.0
Yes	Yes	823	20/10	27.4	88.0	39.7	10.9
No	Yes	823	20/10	4.3	12.6	52.3	2.2

presence of the corona discharge. By enhancement is meant that the combination of catalyst and gas discharge leads to methane conversions and C_2 yields greater than the sum of conversions or yields achieved with catalyst alone and discharge alone. Table 2 summarizes the results of gas discharge promoted catalytic conversion of methane over $Sr–La_2O_3/La(OH)_3$. The greatest enhancement is observed at the lowest temperatures. Under conditions that result in significant enhancement, it was visually observed that the appearance of the discharge over the catalyst qualitatively changes. A significant corona discharge effect is usually accompanied by a pink glow while a poor effect over the regular metal oxides without OH groups is always associated with a blue glow. We speculate that the OH groups on the catalyst surface affect the characteristics of the gas discharge. This effect will be discussed further later.

3.2. Li/MgO

The stable gas discharge effect was achieved over Li/MgO at 873 K as shown in Table 3. No C_2 activity was found with this catalyst in the absence of gas discharge at temperatures less than 973 K. The gas discharge enhancement is thought to be from OH groups present on the catalyst surface. Such OH groups are usually formed by dissociative adsorption of water [19,20]. From Table 3, it is found that the gas discharge enhances greatly the selectivity to C_2 hydrocarbons and to a lesser extent the conversions of methane and oxygen. High reaction temperature should lead to some dehydroxylation of this catalyst which may explain the decreased enhancement at 973 K versus at 873 K.

3.3. CaO/NaOH

A noticeable gas discharge effect over CaO/NaOH was achieved even at 573 K, as shown in Fig. 2. Fig. 2 shows the effect of gas discharge on the selectivity of products at varying temperatures. In our experiments, there are some unidentified products in the liquid condensate but about 20% of the liquid product was formaldehyde. We refer to these products (including formaldehyde) as C_{liq} in all figures of this paper. From Fig. 2, the ethylene selectivity decreases with increasing gas temperature in the low temperature range and then increases slightly above 773 K, while the selectivity of ethane increases with increasing temperature. The maximum C_2 yield occurs at 673 K. These results suggest a change in reaction mechanism or rate limiting steps as the temperature is increased; alternately, thermal catalytic reactions could be important at 673 K in the discharge system due to heating of the catalyst by the discharge. A similar phenomenon was observed over $Sr–La_2O_3/La(OH)_3$ [17]. At low temperatures (below 873 K), the catalyst alone shows essentially no activity for methane conversion. As we previously observed [16], the DC corona discharge is not stable in the absence of the catalyst until the gas temperature reaches around 773 K, and results of the discharge in the absence of catalyst are presented in Fig. 2 only at higher temperatures. The catalyst apparently stabilizes the gas discharge, leading to significant enhancement over catalyst alone or discharge alone, particularly at low temperatures. At high temperatures (e.g., 973 K), the catalyst possesses activity for methane conversion and C_2 product formation, but the enhancement by the gas discharge is still noticeable at 973 K. Compared with results of the catalytic run alone, the methane conversion with the gas

Table 3
Gas discharge promoted catalytic conversion of methane over Li/MgO

Catalyst present	Gas discharge present	Gas temperature (K)	CH_4/O_2	CH_4 conversion (%)	O_2 conversion (%)	C_2 selectivity (%)	C_2 yield (%)
Yes	No	873	20/5	5.4	16.1	0.0	0.0
Yes	Yes	873	20/5	12.1	28.7	77.3	9.4
No	Yes	873	20/5	4.7	21.4	46.3	2.2
Yes	No	973	20/5	7.8	19.6	70.6	5.5
Yes	Yes	973	20/5	11.3	41.2	69.2	7.8
No	Yes	973	20/5	9.1	53.0	34.7	3.2

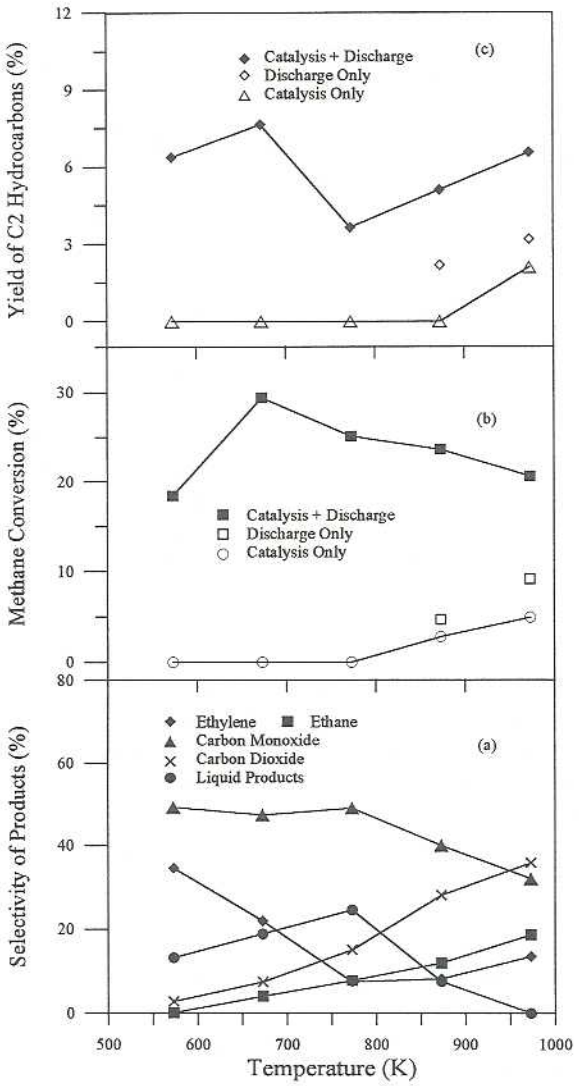

Fig. 2. Effect of temperature on gas discharge promoted catalysis over CaO/NaOH. Total flow rate 100 cm^3/min, CH_4/O_2 ratio 4 : 1, input power 6 W. (a) Selectivities with catalyst plus discharge, (b) methane conversions, (c) yield of C_2 hydrocarbons.

discharge promoted catalysis at 973 K is almost four times higher while the yield for C_2 is over three times larger. The ethylene selectivity at low temperature is much higher than that at high temperature. This means that at low temperatures, the gas discharge promoted catalysis favors ethylene over ethane. Significantly, very little CO_2 is found at low temperatures while the CO yield is high. This result suggests that, particularly at lower temperatures, carbon dioxide may be involved in reactions that are less important at high temperatures.

3.4. NaOH-treated Y zeolites

The experiments over $Sr–La_2O_3/La(OH)_3$, Li/MgO and CaO/NaOH have suggested that OH groups in metal oxide catalysts play an important role in the gas discharge promoted catalytic conversion of methane to higher hydrocarbons. Zeolites can contain very high concentrations of OH groups. The unit cell formula of zeolites can be written as

$$M^{n+}_{x/n}[(AlO_2^-)_x(SiO_2)_y]_z \cdot H_2O$$

where M^{n+} is the cation which balances the negative charge associated with the framework aluminum ions. In addition to the high concentration of OH groups possible on zeolite surfaces, an important characteristic of zeolites is the natural coulombic field formed between the negative charge and cations and/or adsorbed molecules. The presence of such very large electrostatic fields in Y zeolite, which can thus induce reactivity in reactant molecules, has been described in the literature [19,21]. One may expect these electrostatic fields to be modified by a sufficiently strong external electric field or gas discharge. However, such a technique for modifying zeolite activity has been unexplored.

No gas discharge enhancements of catalytic activity were found with Na–ZSM-5 and NH_4Y zeolites, which generated coke quickly. Due to carbon buildup, the corona discharge became unstable in a short time over these zeolites. To reduce the sites' acidity and to increase the concentration of negatively charged sites (and therefore the polarizability of the surface [22]), the Y zeolite was treated with NaOH solution to dissolve part of the silica from NH_4Y zeolite. The comparison of surface atomic compositions before and after the NaOH treatment was presented in Table 1. After NaOH treatment, the surface Si/Al decreases. The total basicities, therefore, are higher than those before NaOH treatment, due to more contributions from oxygen ions of $(AlO_4)^-$ tetrahedra, which exhibit Lewis basicity only. There are insufficient data presently to determine the contribution of the amphiprotic OH groups to the total basicities in the NaOH treated Y zeolite. But, a surprising gas

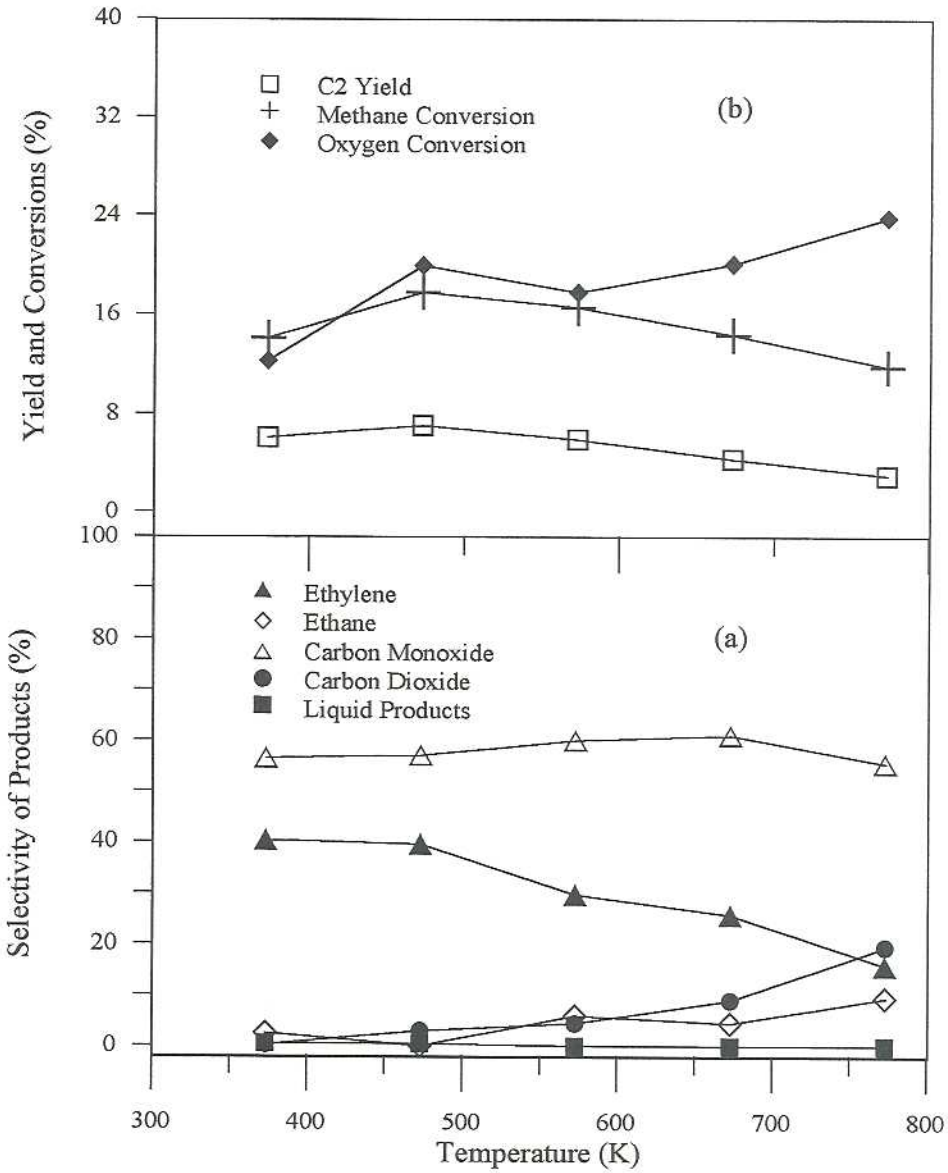

Fig. 3. Effect of temperature on gas discharge promoted catalysis over NaOH-treated Y zeolite. Total flow rate 100 cm^3/min, CH_4/O_2 ratio 4 : 1, input power 6 W. (a) Selectivities, (b) conversions and C_2 yields.

discharge effect over the NaOH treated Y zeolites was achieved. A stable gas discharge enhancement was found at temperatures as low as 373 K. We observed no C_2 activity at any temperature in the absence of gas discharge over the Y zeolites used here, thus the gas discharge greatly modifies the catalytic activity (or the catalyst greatly modifies the corona discharge). The enhancement is shown in Fig. 3. The enhancement is most noticeable at 373 K, at which temperature a very large ethylene/ethane ratio (more than 20 : 1) and a very large CO : CO_2 ratio (about 60 : 1) are observed. Over the entire range of gas temperatures tested here

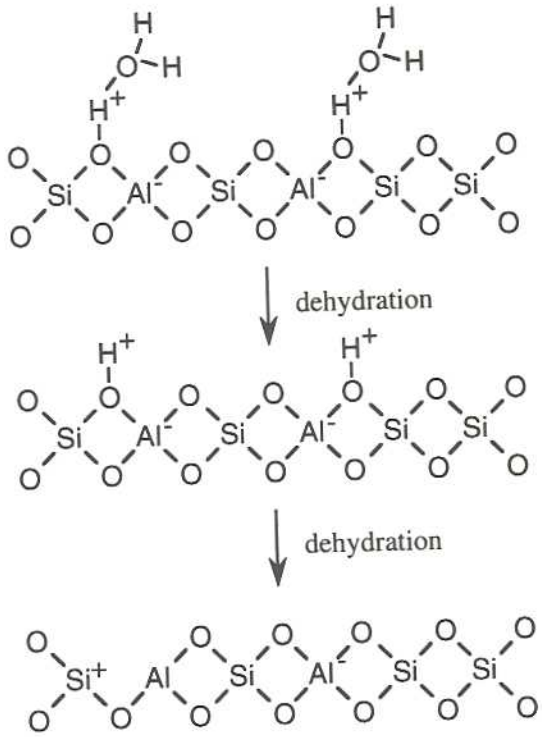

Fig. 4. Dehydration of zeolite.

(373–773 K), the yield of CO_2 is very low while the yield of CO is high. The CO and CO_2 yields and the carbon formation observed under some conditions suggest that carbon dioxide reacts with carbonaceous species to form CO. But it is possible that some CO_2 contributes active oxygen species by electron dissociation attachment reactions [16]:

$$CO_2 + e^- \rightarrow CO + O^- \quad (1)$$

$$CO_2 + e^- \rightarrow CO + O + e^- \quad (2)$$

These reactions provide a source other from molecular oxygen of active oxygen species which enhances methane conversion and/or oxidative dehydrogenation of ethane. We have identified that ethylene is a secondary product formed by dehydrogenation of ethane [16]. The experimental results now suggest that it may be possible to obtain high yields of ethylene and carbon monoxide, two essential chemicals for many industrial applications, by appropriately controlling the electronic energy and gas temperature of the gas discharge. As the basicity of ethylene is higher than that of alkanes, ethylene is more easily adsorbed on zeolite acid sites, and ethylene is a likely coke precursor. Fig. 3 also indicates that there exist some other carbon species C_{liq}, which includes trace formaldehyde, unidentified species, and sometimes carbonaceous deposits. The maximum methane conversion and C_2 yield are obtained at 473 K, and the selectivity of ethylene decreases with increasing temperature. The negative temperature influence on the C_2 yield is thought to be due to dehydration of the zeolites at high temperatures, which results in a decreased OH concentration. The dehydration is shown schematically in Fig. 4. The dehydration also shifts Bronsted acid sites to Lewis acid sites, and these changes result in a decrease in methane conversion.

4. Discussion

4.1. The interactions between the gas discharge and the catalyst

Most electrical energy in a gas discharge goes into the production of energetic electrons, rather than into gas heating, thus gas discharges are a plentiful source of active species for various oxidative or reductive reactions through electron-impact dissociation and ionization reactions [18,23,24]. When the gas discharge is introduced into the catalyst layer, it changes the electronic state of the gas species. Instead of a gas phase consisting of electrically neutral species, electrons, ions and other excited species flow through the catalyst bed. The catalyst particles become electrically charged. The charge on catalyst surfaces, together with other effects of excited species in the gas discharge, leads to variations of the electrostatic potential and work function of the catalyst surface. The chemisorption and desorption performances of the catalyst therefore may be modified [25,26]. The effects of these modifications on methane conversion depend on the amount and concentration of surface charge and the species present on the catalyst surface. An important difference between regular catalysis and the non-equilibrium gas discharge promoted catalysis is the energy distribution between products and the catalyst. In regular catalysis, the temperature of gaseous products is the same as that of the catalyst. For gas

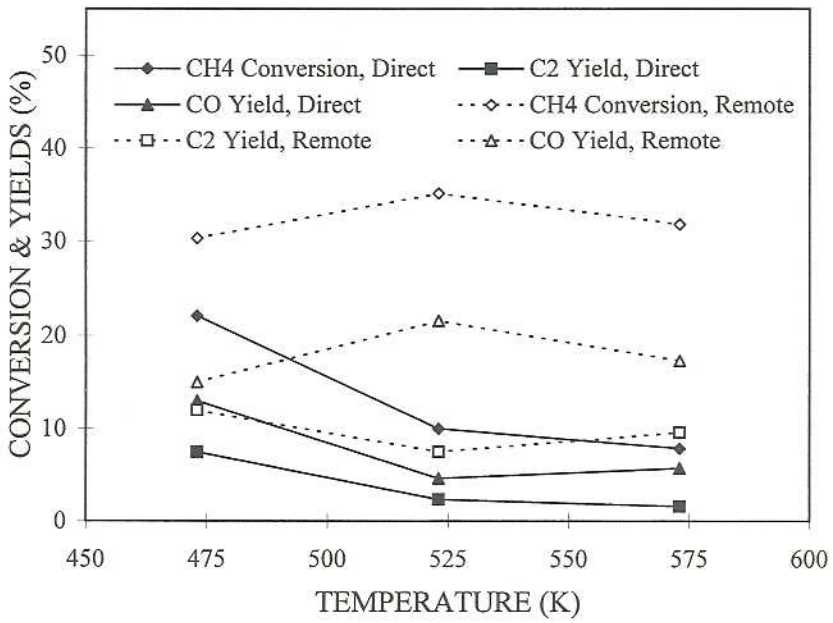

Fig. 5. Comparison of direct and remote corona discharge promoted catalysis over NaOH treated Y zeolite. Total flow rate 100 cm^3/min, CH_4/O_2 ratio 4 : 1, input power 7 W.

discharge promoted catalysis, however, there is an unequal partitioning of the energy between the charged gas species and the catalyst [26–28], with the charged gas molecules having most of the energy. Thus, by acting as a source of charged species, the catalyst may actually enhance the non-equilibrium nature of the gas discharge. We have also observed that in the presence of some solid catalysts, the corona discharge is stable at a lower gas temperature compared to the gas discharge in the absence of the solid catalyst. The color change of the gas discharge with and without the catalyst mentioned above is from the different radiation spectra emitted when the excited species return to the ground state. The important role of the gas discharge can be demonstrated also by the comparison of the remote corona and direct corona discharge promoted catalysis, as shown in Figs. 1 and 5. The remote corona was more effective for methane conversion and C_2 production over the entire range of temperatures used over the NaOH treated Y zeolite. The remote corona provides a larger space for homogeneous gas discharge reactions, while the amount of the catalyst for the direct corona discharge is twice that used for the remote corona. If the heterogeneous reactions contribute more to the total reactions, the direct corona should have more selective products and a higher methane conversion. However, because the greater conversion is observed with the remote corona, we conclude that the gas phase reactions are very important, particularly at low temperatures.

4.2. Radiative effect

When electronically excited states return to the ground state, they emit energy as electromagnetic radiation. Such radiation accounts for the ultraviolet to visible emissions of the gas discharge [24,29]. This radiative decay may have a positive effect on the gas discharge promoted catalytic conversion of methane. It has been shown [30] that O^-, the active oxygen surface species for catalytic OCM, can be produced by UV irradiation of various inorganic oxides. Ozin and Hugues [31] even found that the selective photoactivation of methane can be carried out by UV irradiation of Y zeolites. They proposed that a V-center is formed under UV irradiation:

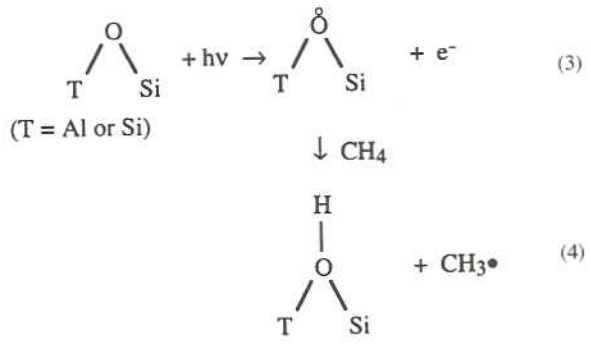

(3)

(4)

The formation of methyl radicals by interaction with the V-center is similar to formation of methyl radicals by interaction with surface O^- [32]. The above reaction was reported at temperatures as low as 298 K.

We propose that a similar process is driven by the radiative decay during the gas discharge promoted catalytic conversion of methane over NaOH treated Y zeolites and other metal oxide catalysts. The photon emitted from radiative decay, can initiate more selective products, but electrons can always be generated at much higher efficiencies than photons, as noted earlier. Therefore, photochemistry is expected to be less important than plasma chemistry for gas discharge promoted catalysis.

4.3. Role of surface OH groups

Evidence exists in the literature for interaction of OH in solids with electric discharges. Solid NaOH and KOH have been used for the catalytic hydrazine synthesis in the presence of a discharge [33]. With intermittent discharge, the yield of hydrazine from ammonia reached approximately 15%. The significant discharge effect was explained by increased adsorption of ammonia due to the intermittent discharge. It has been shown that the introduction of the solid alkali into gas discharge raised the vibrational temperature of gaseous species [33]. Such an increase in the vibrational temperature, for heterogeneous methane conversion, may lead to a more favorable methane chemisorption on catalysts [34–37].

The corona discharge may also induce a charge on the solid catalyst which is related to the strength of the electric field and the dielectric constant of the material [38]. Materials with a strong dipolar character, such as catalysts which are more or less hydrated and contain numerous OH groups, become charged most easily. If the degree of polarization in ionic crystalline hydroxides is excessive, dehydration may occur, leaving behind an oxygen vacancy which may subsequently react to form an active site for methyl radical production [39,40]:

$$M^+[OH]^- \ldots [HO]^- M^+ \rightarrow M^+ + H_2O + O^{2-} + \square + M^+ \quad (5)$$

M^+ represents a metal cation.

Further interaction is possible between the catalyst surface and charged or radical species generated during the discharge. The tendency to form O^- is very high in an oxygen-containing gas discharge due to the electronegativity of oxygen [29]:

$$e^- + O_2 \rightarrow O_2^- \rightarrow O + O^- \quad (6)$$

Besides reacting homogeneously as described above, the active oxygen species O and O^- may react with surface [OH] in the crystal lattice to form a catalytic site active for OCM:

$$2[OH]_s + O \rightarrow O_s + OH \quad (7)$$

or

$$2[OH]_s + O^- \rightarrow O_s + OH^- \quad (8)$$

Finally, when the catalyst surface charge accumulation is sufficient, a microdischarge will be generated in the gaps between the catalyst particles [41]. This microdischarge creates active species in the same fashion as the corona discharge between the electrodes.

At low temperatures (less than 873 K), there exists a large concentration of OH groups on the catalyst. Consequently, the catalyst can be expected to be charged more easily at low than at high temperature. This explains the more significant gas discharge enhancement at low temperatures.

4.4. Reaction mechanisms

In this section, we discuss the steps considered most relevant to explain the observed methane conversion and product selectivities. Most of these steps appear in the literature on methane coupling or the literature related to high temperature reactions. As mentioned above, the OCM reaction is generally considered to include heterogeneous and homogeneous reaction

steps. The catalyst is needed to activate methane by abstraction of a hydrogen from methane to form methyl radicals. We have reported that a corona gas discharge also possesses oxygen species active for the formation of methyl radicals [16]. Methyl radicals can be generated in the gas phase and on the catalyst surface for gas discharge promoted catalytic conversion of methane. Production of C_2 hydrocarbons is believed to occur primarily in the gas phase by coupling of methyl radicals. In our gas discharge promoted catalytic system, no single pathway for methyl radical formation and C_2 hydrocarbon formation can explain all the phenomena observed. In the absence of a gas discharge, all the metal oxide catalysts tested were active for the OCM reaction only at high temperatures. The generally accepted reaction mechanism has been reported in the literature [42,43]. In the absence of a gas discharge, no OCM activity was found at any temperature over Y zeolites. It is believed that for all the catalysts tested here, OH groups play an important role in the heterogeneous methane conversion and possibly for the stabilization of the gas discharge. A complete reaction mechanism for the gas discharge promoted catalytic conversion of methane must include both homogeneous and heterogeneous steps. Although our understanding of the complex reaction mechanism is certainly incomplete, the steps considered most important are presented below.

4.4.1. Homogeneous reaction mechanism

4.4.1.1. Active oxygen species formation and initiation of discharge reactions. The dissociative attachment reaction (Eq. (6)) requires low energy and so is considered most likely for the formation of active species [18,29]. The corona discharge produces electrons with an average electron energy of about 6 eV [18]. This energy is insufficient to directly activate methane because the appearance potentials for methane ions are greater than 12 eV [44]. Because there is a distribution of electron energies, a small fraction of electrons have sufficient energy to activate CH_4 directly, but the direct activation of methane is expected to be a small contribution to methane conversion. Similarly, Lee and Grabowski [45] found no evidence of associative attachment with methane, i.e., formation of CH_4 ions. Active oxygen species may also be formed via direct dissociation reactions between oxygen and electrons, i.e.,

$$\text{Dissociation}: \quad e^- + O_2 \rightarrow 2O + e^- \tag{9}$$

CO_2 and H_2O are products of the gas discharge OCM reaction. The new-formed products CO_2 and H_2O are intrinsically already excited, and require only a relatively low electron energy to dissociate these two molecules [45–47], which may result in further active oxygen species shown below for reactions involving H_2O and in Eqs. (1) and (2) involving CO_2:

$$e^- + H_2O \rightarrow O^- + H_2 \tag{10}$$

$$e^- + H_2O \rightarrow OH^- + H \tag{11}$$

4.4.1.2. Methyl radical formation. O^- has been extensively reported to be the active species for methyl radical formation [45]:

$$O^- + CH_4 \rightarrow CH_3 + OH^- \tag{12}$$

The oxygen species $O(^1D)$ is also known to lead to the formation of methyl radicals [48]:

$$O(^1D) + CH_4 \rightarrow CH_3 + OH \tag{13}$$

4.4.1.3. Hydrocarbon formations. Ethane and ethylene formation [48]. Ethane forms by the reaction of two methyl radicals (Eq. 14), while ethylene probably forms subsequently either by reaction of two ethyl radicals (Eqs. 15 and 16) or by oxidative dehydrogenation of ethane (Eqs. 17 and 18):

$$2CH_3 \rightarrow C_2H_6 \tag{14}$$

$$C_2H_6 + R \rightarrow C_2H_5 + RH \quad (R = H, CH_3, C_2H_5, \ldots) \tag{15}$$

$$C_2H_5 \rightarrow C_2H_4 + H \tag{16}$$

$$2C_2H_5 \rightarrow C_2H_4 + C_2H_6 \tag{17}$$

$$C_2H_6 + O^- \rightarrow C_2H_5 + OH^- \tag{18}$$

$$C_2H_5 + O^- \rightarrow OC_2H_5^- \tag{19}$$

$$\downarrow$$

$$C_2H_4 + OH^-$$

Formaldehyde formation [48,49].

$$CH_3 + O \rightarrow HCHO + H \quad (20)$$

4.4.1.4. H_2O formation [43,50]. The paths by which H_2O and CO_2 are formed are probably many and complex. The following steps exemplify the paths rather than encompass all possible routes. These steps are taken primarily from the literature dealing with high temperature reactions.

$$2OH^- \rightarrow O^{2-} + H_2O \quad (21)$$

$$OH + RH \rightarrow H_2O + R \quad (R = H, CH_3, C_2H_5, \ldots) \quad (22)$$

$$H_2 + O \rightarrow H_2O \quad (23)$$

4.4.1.5. CO_x formation [48,49].

$$CH_3 + O_2 \rightarrow OH + H_2CO \quad (24)$$

$$H_2CO + R \rightarrow HCO + RH \quad (R = H, CH_3, C_2H_5, \ldots) \quad (25)$$

$$HCO \rightarrow H + CO \quad (26)$$

$$OH + CO \rightarrow CO_2 + H \quad (27)$$

$$H_2CO + OH \rightarrow HCO + H_2O \quad (28)$$

$$CH_3 + HCO \rightarrow CH_4 + CO \quad (29)$$

The effects of temperature, residence time and feed methane to oxygen ratio on the methane conversion and C_2 yield in the homogeneous corona discharge reactions have been presented earlier [16].

4.4.2. Heterogeneous reaction mechanism

4.4.2.1. Metal oxide catalysts. The heterogeneous reactions occurring in the presence of a gas discharge depend on the gas temperature. At low temperatures, the catalysts used here have little or no intrinsic activity. The active oxygen species on the catalyst are formed via reactions (5), (7) and (8). Additional active sites could be created by the radiation effect. Adsorbed or gas phase methane reacts with these active oxygen species to generate methyl radicals, which produce C_2 hydrocarbons in the gas phase.

At high temperature, some of the catalysts used here do show C_2 activity even in the absence of the discharge, and this "intrinsic" activity contributes to methane conversion and C_2 production in the presence of the discharge. The intrinsic catalytic activity and the gas discharge promoted catalytic activity should both be taken into account in a complete reaction mechanism. The intrinsic catalytic reaction mechanism is discussed extensively in the literature [42,43].

4.4.2.2. NaOH-treated Y zeolites. The situation is somewhat different over the NaOH treated Y zeolites. These catalysts demonstrate no selectivity for C_2 hydrocarbons even at very high temperatures, thus no "intrinsic" catalytic reaction mechanism need be considered. The radiation effect (reactions (3) and (4)) may contribute to methyl radical production, but the photochemical efficiency is generally much less than that of the electronic process as noted earlier. The observed activity may be related to the interaction of the charged particles with the extant electric field in the zeolite pores, or to a modification of the electric field in the pores by the charging of the catalyst particles. The interaction or modification may significantly change the Bronsted and/or Lewis acidity of sites on the catalyst. It was also noted that as the temperature was increased (causing dehydration and a shift from Bronsted to Lewis behavior), the C_2 selectivity and even the methane conversion decreased, suggesting an important role of Bronsted behavior in the observed reactions.

5. Conclusions

The results presented here suggest that the polarized OH groups play an important role in gas discharge promoted catalytic conversion of methane to higher hydrocarbons. The gas discharge enhancement depends on the temperature, the concentration of OH groups and probably the acidity or basicity of the OH site. The most significant gas discharge effect was achieved at low temperatures, as low as 373 K over the NaOH treated Y zeolite. Notably, the gas discharge promoted catalysis produces little CO_2, especially over NaOH treated Y zeolite. There exists the potential for gas discharge promoted catalysis to produce ethylene from methane with high selectivity to ethylene with the only significant other carbon containing products CO and ethane.

Acknowledgements

Support from the US Department of Energy (under contract #DE-FG21-94MC31170) is greatly appreciated. We are grateful to Micromeritics for the donation of the ASAP 2100 used for surface area measurements. Appreciation is extended to Dr. Daniel Resasco at the University of Oklahoma and to Prof. Genhui Xu, Prof. Hongfang Chen and Prof. Xien Xu at Tianjin University, Tianjin, China for their valuable suggestions. Dr. Daniel Resasco also kindly provided us with the Na–ZSM-5 catalyst. We thank also Ms. Fie He at Tianjin University for her assistance in XPS analysis and Dr. Barry Weaver at the University of Oklahoma and Prof. Sicheng Liang at Tianjin University for their assistance with XRD characterization. Moreover, we thank Mr. Bobby Hill and Mr. Yeoh Heanchin at the University of Oklahoma for experimental work.

References

[1] T. Ito, J.H. Lunsford, Nature 314 (1985) 721.
[2] D.J. Driscoll, W. Wilson, J.X. Wang, J.H. Lunsford, J. Am. Chem. Soc. 107 (1985) 58.
[3] J.A. Roos, A.G. Bakker, H. Bosch, J.G. Van Ommen, J.R.H. Ross, Catal. Today 1 (1987) 133.
[4] J. Kiwi, K.R. Thampi, N. Mouaddib, M. Grutzel, Catal. Lett. 18 (1993) 15.
[5] X.-H. Li, K. Fujiimoto, Chem. Lett. (1994) 1581.
[6] P. Pereira, S.H. Lee, G.A. Somorjai, H. Heinemann, Catal. Lett. 6 (1990) 255.
[7] J. Rasko, P. Pereira, G.A. Somorjai, H. Heinemann, Catal. Lett. 9 (1991) 395.
[8] Y.F. Chang, G.A. Somorjai, H. Heinemann, J. Catal. 141 (1993) 713.
[9] H.G. Ma, S.H. Zhong, Abstract of Sixth National Symposium on Catalysis, Shanghai, 1992, p. 316.
[10] C.-L. Chen, P.-J. Hong, S.-S. Dai, J.-D. Kan, J. Chem. Soc. Faraday Trans. 91 (1995) 1179.
[11] S.J. Suib, R.P. Zerger, J. Catal. 139 (1993) 383.
[12] Z.-L. Zhang, X.E. Verykios, M. Baerns, Catal. Rev. Sci. Eng. 36 (1994) 507.
[13] W.-Y. Tung, L.L. Lobban, Ind. Eng. Chem. Res. 31 (1992) 1621.
[14] S.C. Bhumkar, L.L. Lobban, Ind. Eng. Chem. Res. 31 (1992) 1856.
[15] B. D. Ajmera, The oxidative coupling of methane on $Sr_{0.1}La_{0.9}O_3$ catalyst, MS Thesis, The University of Oklahoma, 1995.
[16] C.-J. Liu, A. Marafee, B. Hill, G.-H. Xu, R. Mallinson, L.L. Lobban, Ind. Eng. Chem. Res. 35 (1996) 3295.
[17] A. Marafee, C.-J. Liu, G.-H. Xu, R. Mallinson, L.L. Lobban, Ind. Eng. Chem. Res. 36 (1997) 632.
[18] B. Eliasson, U. Kogelschatz, IEEE Trans. Plasma Sci. 19 (1991) 1063.
[19] B.C. Gates, Catalytic Chemistry, Wiley, New York, 1991, p. 254.
[20] I. Balint, K.-I. Aika, J. Chem. Soc. Faraday Trans. 91 (1995) 1805.
[21] G.C. Bond, Heterogeneous Catalysis: Principles and Applications, Clarendon Press, Oxford, 1974, p. 38.
[22] J.A. Rabo, G.J. Gajda, Catal. Rev. Sci. Eng. 31 (1989–1990) 385.
[23] J. Chang, P.A. Lawless, T. Yamamoto, IEEE Trans. Plasma Sci. 19 (1991) 1152.
[24] A. von Engel, Ionized Gases, Oxford University Press, London, 1965.
[25] V.N. Ageev, Progress in Surface Science 47 (1994) 55.
[26] D.E. Rapakoulias, S. Cavadias, D. Mataras, J. High Temp. Chem. Proc. 2 (1993) 231.
[27] D.E. Rapakoulias, A. Giequel, M.P. Bergougnan, J. Amouroux, Rev. Phys. Appl. 17 (1982) 95.
[28] J.C. Tully, J. Chem. Phys. 73 (1980) 6333.
[29] A. Grill, Cold Plasma in Materials Fabrication, IEEE Press, New York, 1993, p. 49.
[30] S.L. Kalinguine, B.N. Shelimov, V.B. Kazansky, J. Catal. 49 (1978) 384.
[31] G.A. Ozin, F. Hugues, J. Phys. Chem. 86 (1982) 5174.
[32] K. Aika, J.H. Lunsford, J. Phys. Chem. 81 (1977) 1398.
[33] M. Venugopalan, S. Vepek, in: F.L. Boschke (Ed.), Topics in Current Chemistry: Plasma Chemistry IV; Kinetics and Catalysis in Plasma Chemistry, Springer, New York, 1983.
[34] C.N. Stewart, G. Erlich, J. Chem. Phys. 62 (1975) 4672.
[35] H.F. Winters, J. Chem. Phys. 64 (1976) 3495.
[36] C.T. Rettner, H.F. Pfnuf, D.J. Auerbach, J. Chem. Phys. 84 (1986) 4163.
[37] S.G. Brass, D.A. Reed, G. Erlich, J. Chem. Phys. 70 (1979) 5244.
[38] G.B. Nichols, IEEE Trans. Ind. Appl. 1A-13 (1977) 74.
[39] S. Lacombe, C. Geantet, C. Mirodatos, J. Catal. 151 (1994) 439.
[40] P.J. Durrant, B. Durrant, Introduction to Advanced Inorganic Chemistry, Wiley, New York, 1962, p. 371.
[41] T. Yamamoto, K. Ramanathan, P.A. Lawless, D.S. Ensor, J.R. Newsome, N. Plaks, G.H. Ramsey, IEEE Trans. Ind. Appl. 28 (1992) 528.
[42] O.V. Krylov, Kinet. Catal. 34 (1993) 11.
[43] E.N. Voskresenskaya, V.G. Roguleva, A.G. Anshits, Catal. Rev. Sci. Eng. 37 (1995) 101.
[44] S.L. Sorensen, A. Karawajczyk, C. Stromholm, M. Kirm, Chem. Phys. Lett. 232 (1995) 554.
[45] J. Lee, J.J. Grabowski, Chem. Rev. 92 (1992) 1611.
[46] P.J. Chantry, J. Chem. Phys. 57 (1972) 3180.
[47] O.J. Orient, S.K. Strivastava, Chem. Phys. Lett. 96 (1983) 681.
[48] A. Oumghar, J.C. Legrand, A.M. Diamy, N. Turillon, Plasma Chem. and Plasma Processing 15 (1995) 87.
[49] E.E. Brock, P.E. Savage, AIChE J. 41 (1995) 1874.
[50] D.A. Parkes, J. Chem. Soc. Faraday Trans. 1(68) (1972) 2103.